Chalcogenide Letters Vol. 16, No. 4, April 2019, p. 163 - 173

# EFFECT OF Cr DOPING INTO CdSe HOST NANOSIZE THIN FILMS ON THE STRUCTURAL, OPTICAL AND MAGNETIC PROPERTIES

H. H. HEGAZY[a, b], E. R. SHAABAN[b*], M. REBEN[c]
[a]*Physics Dept., Faculty of Science, King Khalid University, P.O. Box 9004, Abha, Saudi Arabia*
[b]*Physics Dep., Faculty of Science, Al- Azhar University, Assiut branch, Assiut, 71542 Egypt.*
[c]*Faculty of Materials Science and Ceramics, AGH - University of Science and Technology, al. Mickiewicza 30, Cracow, 30-059, Poland*

Different composition of $Cd_{1-x}Cr_xSe$ (x = 0, 0.02, 0.04, 0.06, 0.08, and 0.10) films were evaporated by electron beam gun. The effect of Cr doping on the structural, optical, and magnetic properties have been investigated. X-ray diffraction studies confirm the formation of wurtzite structure for all $Cd_{1-x}Cr_xSe$ films. The lattice constants are found to be increased with increasing Cr concentration. The crystallite size increases and the lattice strain decreases with the increase in Cr content. The elemental constituents were characterized by energy dispersive X-ray. Both the refractive index and film thickness have been determined using the envelop method suggested by Swanepoel. Optical studies showed a decrease in refractive index and an increase in energy gap with the increase of the Cr doping. Magnetization measurements via vibrating sample magnetometer showed a hysteresis loop and confirmed room temperature ferromagnetism in Cr-doped CdSe films. The change in Optical constants, energy gap, and magnetic properties, which have been deduced can be interpreted in terms of micro structural parameters.

(Received March 5, 2019; Accepted April 12, 2019)

*Keywords:* $Cd_{1-x}Cr_xSe$ thin films, Zinc blend wurtzite, Optical constants, Energy gap, Hystersis loop

## 1. Introduction

Semiconductors of II-VI films such as CdSe, ZnTe CdS, CdTe are characterized by their wide band gap [1]. Therefore they have many applications in photovoltaic solar cells and optoelectronics devices. CdSe is n-type semiconductor thin films with a direct optical energy gap of about 1.75 eV. CdSe films are widely used for optoelectronic devices fabrication [2] such as solar cells [3, 4], light emitting devices [5], lasers [6], photo detectors [7] and thin film transistors [8]. Additional a small amount of magnetic transition metal impurities to the host semiconducting materials to obtain dilute magnetic semiconductors (DMS). DMS represents potential resources for spintronic devices [9-11]. It is an exciting field of research wherein both the charge and spin are used for transportation, storage, and processing of information in a single spintronic device [12]. Room temperature ferromagnetism (RTFM) is an essential property for DMS materials. In order to acquire RTFM in DMS materials, transition metal (Fe, Ni, Co, Mn, Cr) has been doped in different semiconductors such as ZnO [13], GaN [5], TiO2 [6], CdS [14], CdSe [15] and SnO2 [16]. II-VI and III-V DMS offer a unique combination of structural, electronic, optical and magnetic properties, which strongly depends on the nature and concentration of the dopant. The transition metals find greater solubility in II–VI compound semiconductors when compared with III-VI semiconductors[17].Among II–VI semiconductors, cadmium selenide (CdSe) is a well-known semiconductor, crystallizing in either the wurtzite or the zinc blende structure [18-23]. It has

*Corresponding author: esam_ramadan2008@yahoo.com

suitable properties for applications in electronics and optoelectronic devices such as laser diodes, high efficiency solar cells, sensors, and biomedical imaging devices [24-27]. In the present investigation, we have synthesized Cr doped CdSe powders via solid state reaction by varying the chromium concentration.

In the presented work chromium as transition metal with different concentrations was doped in CdSe by the solid-state method and the resulted samples were deposited on glass substrates as a thin film. The primary target of this study is to compose CdSe samples in which the chromium doping is not affecting its crystal structure but at the same time become a room temperature ferromagnetic DMS. Also, the optical properties of the obtained Cr-doped CdSe were investigated, with a blue shift in the optical band gap with dopant increase. Also, studies on the magnetic properties of $Cd_{1-x}Cr_xSe$ were reported. The change in Optical constants, energy gap, and magnetic properties, which have been deduced can be interpreted in terms of micro structural parameters.

## 2. Experimental procedures

Different composition of $Cd_{1-x}Cr_xSe$ (x = 0, 0.02, 0.04, 0.06, 0.08, and 0.10) powders were prepared by a conventional solid-state reaction method. Using ball milling technique, Stoichiometric amounts of high–purity (99.999%) analytical grade CdSe and CrSe powders purchased form (M/S Sigma-Aldrich Co) were mixed in a ball mortar for about 30 min according to the following reaction:

$$xCrSe + (1-x)CdSe \rightarrow Cd_{1-x}Cr_xSe \quad (1)$$

The mixed powders were then pressed into a disk–shape pellet. Such pellets were used as the starting materials from which the thin film will be prepared; the same technique was proposed for a different compound in our previous studies [17-20]. Thin films of $Cd_{1-x}Cr_xSe$ were deposited onto glass substrates maintained at 400 K. The pellets of $Cd_{1-x}Cr_xSe$ were evaporated using the electron beam gun (Edward Auto 306) from a heat resistive quartz crucible onto dried pre–cleaned glass substrates (25 mm x 25 mm) at a pressure of about $10^{-6}$ Pa. During the evaporation process, the thickness of the produced films was monitored using FTM6 thickness monitor. The thicknesses of the as–deposited films were fixed at 500 nm at different compositions, and the deposition rate was adjusted at 2 nm/sec. Such a low deposition rate produces a film composition, which is very close to that of the bulk starting material [21, 22]. The substrates were rotated at a slow speed of 5 rpm, to obtain a homogenous and smooth film. X–ray powder diffraction (XRD) Philips diffractometry (1710), with Cu–$K_\alpha$ radiation ($\lambda$ = 1.54056 Å) has been used to examine the phase purity and crystal structure of $Cd_{1-x}Cr_xSe$ 2$\theta$ ranged between 5° and 70° with step–size of 0.02° and step time of 0.6 seconds. The compositional analysis was carried out using energy dispersive X-ray spectroscopy (EDAX). The relative error of determining the indicated elements does not exceed 2 %. The optical measurements were performed from spectral transmittance and reflectance in the range of 300-2500 nm taken at the normal incident by double beam spectrophotometer (JASCO, V-670). The magnetic properties of the prepared films were studied using the vibrating sample magnetometer model (VSM-9600M-1, USA). The measurements were conducted at room temperature in a maximum applied field of 15 kOe.

## 3. Results and discussion

### 3.1. X-ray diffraction and morphological analysis

Rietveld refinement is a technique for use in the characterization of crystalline materials [28]. The X-ray diffraction of powder samples results in a pattern characterized by reflections (peaks in intensity) at certain positions. The height, width, and position of these reflections can be used to determine many aspects of the material's structure. The Rietveld method uses a least

squares approach to refine a theoretical line profile until it matches the measured profile. Fig. 1 illustrates Rietveld refinement for CdSe powder sample. All the diffraction peaks perfectly match with the standard JCPDS data (00-2- 330) for CdSe system exhibiting wurtzite structure. No traces of chromium metal clusters or oxides were observed in XRD patterns.

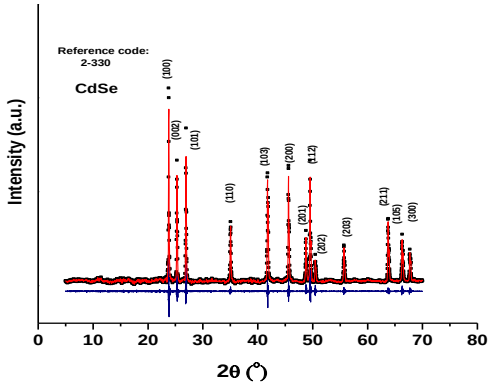


*Fig. 1. Rietveld refinement of CdSe powder sample.*

Fig. 2 exhibits the sharp diffraction line of the preferred crystalline orientation (002) that indicating a good crystallinity of the prepared thin films. There are significant shifts to lower angles of the (002) peaks for the films with incorporating Cr at the expense of Cd in $Cd_{1-x}Cr_xSe$ thin films (clearly shown in Fig. 3). This shift may be attributed to, the atomic radius of the Cr atom (0.63 Å) is smaller than the atomic radius of Cd atom (0.97 Å) [23, 24].

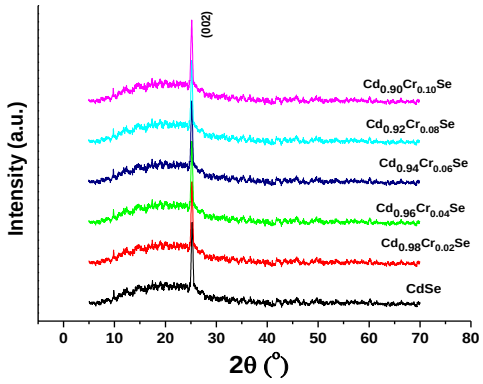


*Fig. 2. XRD patterns of $Cd_{1-x}Cr_xSe$ thin films on glass substrates.*

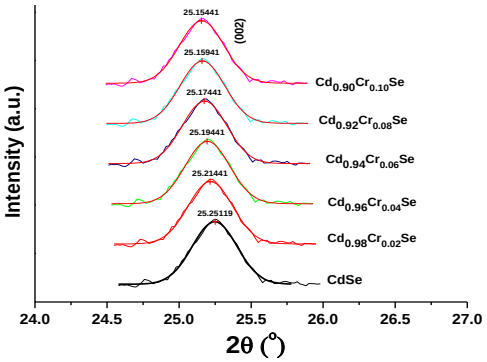


*Fig. 3. Magnified (200) XRD peak of $Cd_{1-x}Cr_xSe$ thin films.*

The hexagonal crystals are characterized by two lattice parameters, a and c, and the interplanar is given by [25]:

$$\frac{1}{d_{hkl}^2} = \frac{4}{3}\frac{h^2 + hk + k^2}{a^2} + \frac{l^2}{c^2} \tag{1}$$

Where *hkl* are Miller indices of the plane. The interplanar spacings $d_{hkl}$ for these thins films were calculated from Bragg's law [29]

$$\lambda = 2d_{hkl}\sin\theta \tag{2}$$

where $\lambda$ is the X-ray wavelength of Cu-$K_\alpha$ radiation ($\lambda$ = 1.54056 Å), and $\theta$ is the Bragg's diffraction angle of the peak.

The lattice constants 'a' and 'c' of the $Cd_{1-x}Cr_xSe$ films were calculated from XRD data using the following simple equations

$$a = b = \lambda\left(\sqrt{3}\sin\theta\right)^{-1} \tag{3-a}$$

and

$$c = \lambda\left(\sin\theta\right)^{-1} \tag{3-b}$$

The lattice constants are found to be increased with increasing Cr concentration as shown in Fig. 3. These results imply that the $Cr^{2+}$ has been incorporated into the crystal lattice of CdSe by replacing Cd in CdSe lattice, which produces a strain in the host lattice Similar variation of lattice constant with dopant was observed by the authors in Cu doped CdSe [24] and Cr doped ZnTe [25].

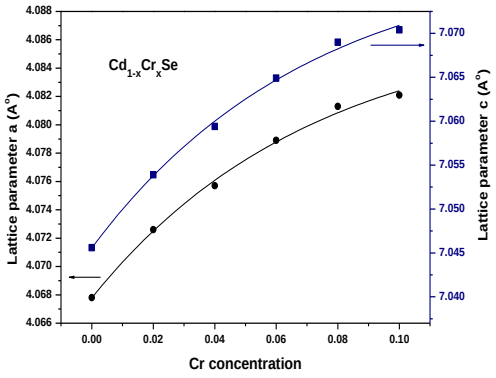


*Fig. 4. Hexagonal Lattice parameters "a" and "c" as a function of Cr concentration for $Cd_{1-x}Cr_xSe$ thin films.*

In terms of XRD analysis, the microstructure parameters both the lattice strain and crystallites size can be estimated. The lattice strain ($\varepsilon$) is calculated using the following equation (30-32):

$$\varepsilon = \frac{\beta}{4\tan(\theta)} \tag{4}$$

where $\beta$ is the full width at half maximum (FWHM), that can be calculated using the following relation (33, 34):

$$\beta = \sqrt{\beta_{obs}^2 - \beta_{std}^2} \tag{5}$$

Where $\beta_{obs}$ is the integral peak profile width of the sample and where $\beta_{std}$ is the peak broadening due to the instrument which is the measured FWHM for a pure standard sample, in our measurement we used pure silicon (~ 99.9999 %) as an internal standard. Using the Scherrer's formula, crystal size $D_v$ was calculated using the following equation (35, 36):

$$D_v = \frac{0.89\lambda}{\beta \cos(\theta)} \tag{6}$$

Both lattice strain and crystallites size of the pure and Cr-doped CdSe films are plotted as functions of Cr content (Fig. 5). It was found that, the crystallite size increases and the lattice strain decrease, with the increasing in Cr content in $Cd_{1-x}Cr_xSe$ thin films.

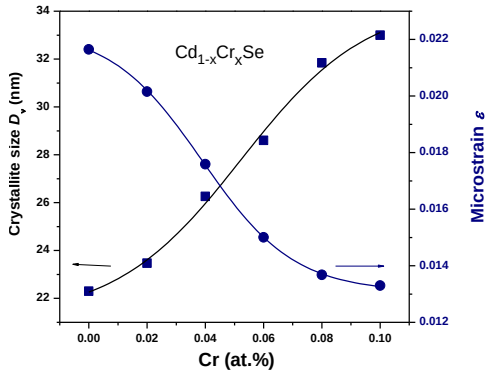


*Fig. 5. Crystallite size and microstrain as functions of Cr content of $Cd_{1-x}Cr_xSe$ thin films.*

It means that an inversely proportional relation between crystallite size and lattice strain that may be attributed to the decreasing of the lattice volume. It is revealed that the lattice strain of the $Cd_{1-x}Cr_xSe$ films decreases with the increase in Cr concentration. The ionic radii of the $Cr^{2+}$ ion (0.063 nm) being smaller as compared to $Cd^{2+}$ ion (0.097 nm) occupying hexagonal sites which leads to a decrease in lattice volume and contract the unit cell, therefore, decrease the lattice strain (37, 38). The recognized increase in the crystallite size and decrease in the lattice strain is also attributed to the lowering in the imperfection of CdSe with Cr addition.

Fig. 6 (a, b) shows the EDAX spectra of for both $Cd_{0.96}Cr_{0.04}Se$ and $Cd_{0.90}Cr_{0.10}Se$ films, which proves the existence of Cd, Se, and Cr. The findings are in good agreement with the chemical composition of the intended to be made the sample. The Cr peak is observed in the EDAX spectra, which suggests that $Cr^{2+}$ has successfully doped in the lattice of CdSe.

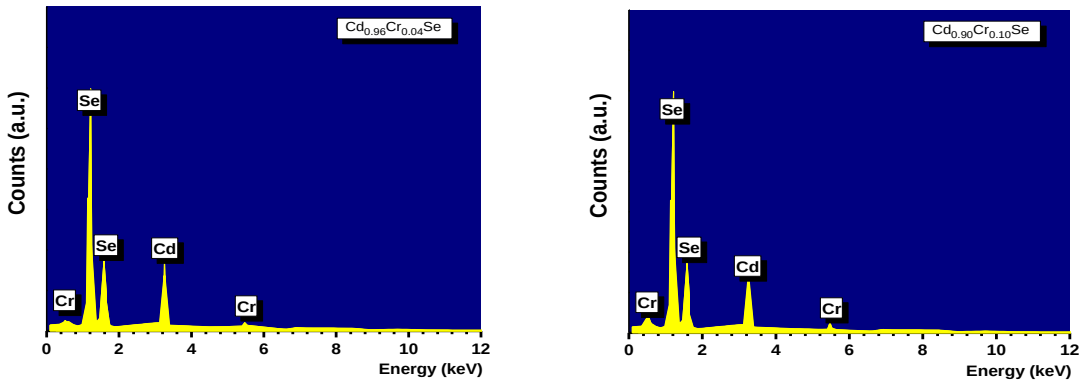


*Fig. 6. EDAX of (a) $Cd_{0.96}Cr_{0.04}Se$ and (b) $Cd_{0.90}Cr_{0.10}Se$ films.*

### 3.2. Optical properties

The double beam spectrophotometer was adopted to measure the transmittance, *T*, and reflectance, *R* in wavelength range extended from 400 to 2500 nm for different composition of $Cd_{1-x}Cr_xSe$ (x = 0, 0.02, 0.04, 0.06, 0.08, and 0.10) films as shown in Fig. 7. This figure shows that the absorption edge shifted towards lower wavelength with increasing the Cr at the expense of Cd.

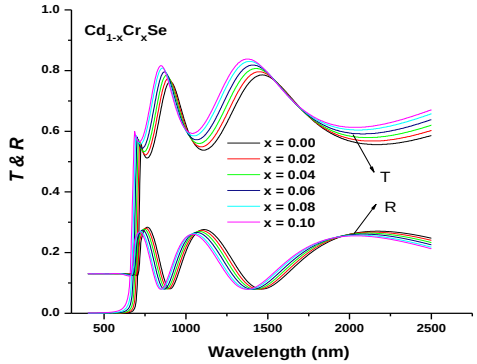


*Fig. 7. Transmittance and reflectance spectra for $Cd_{1-x}Cr_xSe$ thin films with different Cr contents.*

The refractive index (*n*) is an important parameter, which is an essential property for practical applications. It is associated with the electronic polarizability of ions as well as the electric field within the material. The refractive index of the investigated films is calculated utilizing the experimentally measured transmission data by the envelope method which has been suggested by Swanepoel [26, 27]. Fig. 8 shows the application of the envelope method on the optical transmittance $T_\lambda$ of CdSe thin films as an example. The same procedures were used for the data measured at other different composition of $Cd_{1-x}Cr_xSe$ films. Based on the Swanepoel method, the refractive index (*n*) can be deduced at any wavelength from the following formula **[**37, 38]

$$n = [N + (N^2 - s^2)^{1/2}]^{1/2} \tag{7}$$

where

$$N = 2s\frac{T_{Min} - T_{\min}}{T_{Min}T_{\min}} + \frac{s^2+1}{2} \quad , \quad s = \frac{1}{T_s} + \left(\frac{1}{T_s^2}\right)^{1/2} \tag{8}$$

Where, $T_{Max}$ and $T_{min}$ are the interference fringes maxima and minima, respectively; $T_s$ and s is the transmittance and refractive index of the substrate. The variation of refractive index (*n*) of different compositions $Cd_{1-x}Cr_xSe$ thin films with the wavelength of the incident photon is shown in Fig. 9.

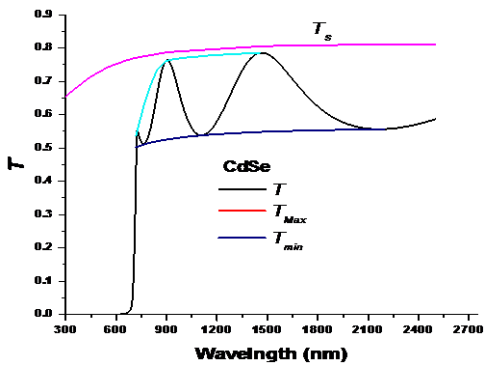


*Fig. 8. The typical transmittance spectra of CdSe thin film with the $T_s$ , $T_{Max}$ and $T_{min}$ curves.*

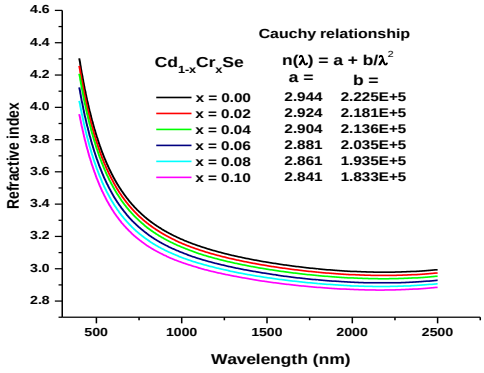


*Fig. 9. The spectral dependence of refractive index n of $Cd_{1-x}Cr_xSe$ thin films with different Cr contents.*

Moreover, if $n_{e1}$ and $n_{e2}$ are the refractive indices at two adjacent maxima (or minima) at $\lambda_1$ and $\lambda_2$, it follows by the expression gives the film thickness

$$d = \frac{\lambda_1 \lambda_2}{2(\lambda_1 n_{e2} - \lambda_2 n_{e1})} \tag{9}$$

The values of film thickness were about 450 ± 2% nm for all thin films. Furthermore, the values of $n$ can be fitted using the two term of Cauchy dispersion relationship, $n(\lambda) = a + b/\lambda^2$, which can be used for extrapolation the whole regions of wavelengths [39-41] as shown in Fig. 9. In terms of the least squares fit of the two sets of values of $n$ for the different compositions of $Cd_{1-x}Cr_xSe$ thin films are illustrated at the inset of Fig. 9. Fig. 11 shows that the refractive index decreases with increasing Cr content, over the entire spectral range, studied.

The absorption coefficient ($\alpha$) can be obtained in the strong absorption region of the experimentally measured values of $R$, $T$, and $d$ according to the following expression [38-44]:

$$\alpha = \frac{1}{d} \ln \left[ \frac{(1-R)^2 + \left[ (1-R)^4 + 4R^2T^2 \right]^{1/2}}{2T} \right] \tag{10}$$

The nature of transition, direct or indirect, is given according to the relation [38-45]:

$$\alpha(h\nu) = \frac{K(h\nu - E_g^{opt})^n}{h\nu} \tag{11}$$

where $K$ is a constant, which depends on the transition probability and is $E_g^{opt}$ the optical band gap, and the exponent 'n' depends upon the type of transition.

Fig. 10 shows a proper fitting of $(\alpha h\nu)^2$ versus photon energy ($h\nu$) for $Cd_{1-x}Cr_xSe$ thin films. The values of the optical band gap $E_g^{opt}$ were taken as the intercept of $(\alpha h\nu)^2$ versus ($h\nu$) at $(\alpha h\nu)^2 = 0$ for the allowed direct transition. The optical band gap derived for each film is shown in Fig. 12. As shown in Fig. 12, the estimated optical band gap found to be increased with increasing the Cr content. The increasing in optical band gap may be attributed to **the first** is the increasing in crystallite size with increasing the Cr content. When photons are incident on the semiconductor material, they will be absorbed only when the minimum energy of photons is enough to excite an electron from the valence band to the conduction band or when the photon energy equal to the energy gap of the material. The prepared nanoparticles are highly confined, and the absorption spectrum of it becomes more structured because of its electronic band structure changes to

molecular level with non-vanishing energy spacing. So, the material needs more energy for the electronic transition from valence band to conduction band. Hence the band gap energy of nanoparticles is more than that of the bulk. **The second** is as the particle size reaches the Nano scale, where every particle is made up only a minimal number of atoms, the number of overlapping of orbitals or energy level decreases and the width of the band gets narrow. As a result, it will cause an increase in the energy gap between the valance band and the conduction band.

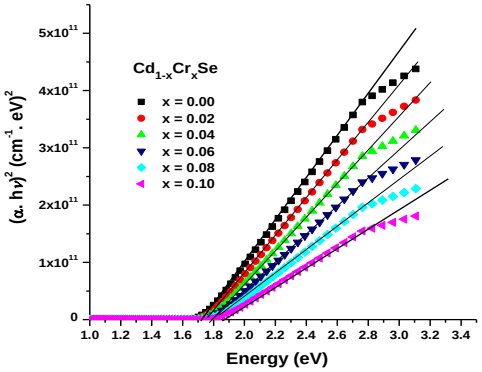


*Fig. 10. Variation of $(\alpha.h\nu)^2$ vs. $h\nu$ for $Cd_{1-x}Cr_xSe$ thin films with different Cr contents.*

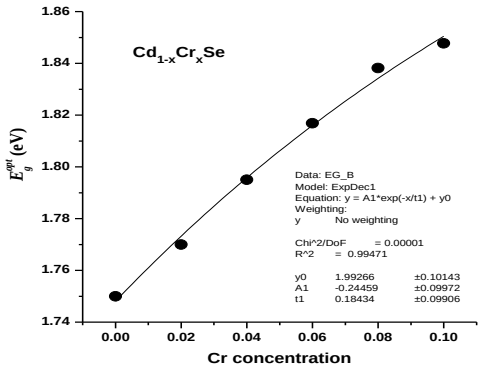


*Fig. 11. Energy gap against Cr concentration of $Cd_{1-x}Cr_xSe$ thin films.*

### 3.3. Magnetic properties

The magnetic properties of $Cd_{1-x}Cr_xSe$ (x = 0, 0.02, 0.04, 0.06, 0.08, and 0.10) thin films were studied by applying the magnetic fields parallel to the film planes. The magnetization measurements *M(H)* against the magnetic field (hysteresis *M-H* curves) of $Cd_{1-x}Cr_xSe$ thin films are shown in Fig. 13. All the data were obtained after the removal of the diamagnetic contribution from the glass substrates. The magnetization curve of pure CdSe (x = 0), shows a diamagnetic-like behavior as expected from its intrinsic diamagnetic nature, similar to previous studies (46, 47). With a negative magnetic susceptibility (80). However, at a lower magnetic field value, weak ferromagnetism has been observed in CdSe thin film in the order nano crystallize size scale, a similar observation has been confirmed by Sundaresan and Rao [48]. For CdSe nanoparticles.

The *M-H* curves at room temperature for doped $Cd_{1-x}Cr_xSe$ films (x = 0, 0.02, 0.04, 0.06, 0.08, and 0.10) in Fig. 13, show a hysteresis behavior, revealing a ferromagnetic characteristic with a small coercive field and low remanence displayed soft ferromagnetism. The magnetism in doped CdSe nanoparticles may be originated possibly from carrier mediated exchange interactions between delocalized carriers of the host and the localized *d* spins of the Cr ions. The same behavior has been observed in Co doped CdSe [49, 50].

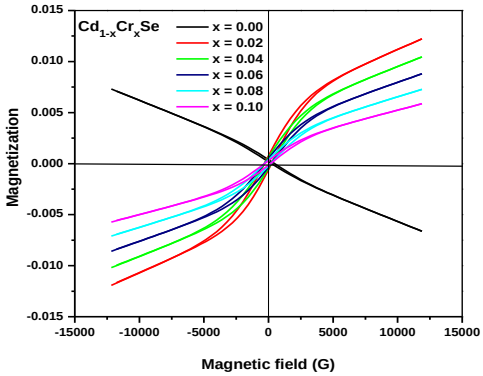


*Fig. 12. M-H hysteresis curves of $Cd_{1-x}Cr_xSe$ thin films.*

The magnetic parameters could be extracted from the hysteresis *M-H* curves, such as the relative the remanent magnetization ($M_r$) and the coercive field ($H_c$) for all $Cd_{1-x}Cr_xSe$ films. These magnetic parameters were shown in Fig. 13. The curves show that as the Cr content in the $Cd_{1-x}Cr_xSe$ nanocrystalline thin films increase, these magnetic parameters continuously increase. The ferromagnetic loop is not saturated for all $Cd_{1-x}Cr_xSe$ nano thin films.

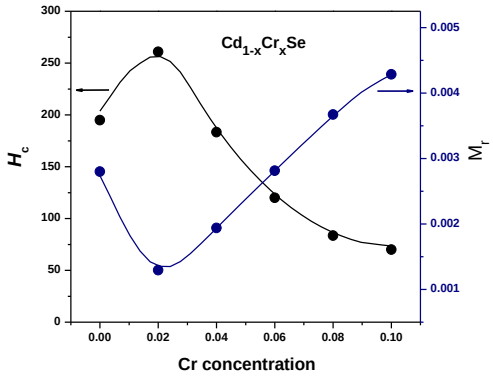


*Fig. 13. The dependence of the coercive field ($H_c$) and the remanent magnetization ($M_r$) for $Cd_{1-x}Cr_xSe$ films with different Cr contents.*

Cr doped CdSe with small percentage till 10 % represent magnetic semiconductor (DMS) and Ferromagnetism source in (DMS) is still a controversial not fully understood argument. However, two specific mechanisms derived from several theories are frequently proposed to explain DMSs ferromagnetism; the bound magnetic polarons (BMPs) that produce long-range magnetic order [51, 52], or the carrier induced exchange interaction of Ruderman-Kittel-Kasuya-Yosida, (RKKY interaction) [53, 54]. To investigate the origin of ferromagnetism in Cr-doped CdSe films in the presented work, we propose two possibilities. The first possibility could be due to the micro Cr clusters. However, the XRD measurements reveal no Cr clusters. Due to the antiferromagnetic nature of Cr, the observed ferromagnetism cannot be the result of metal clusters nor impurity phases. The second probability is the carrier-induced ferromagnetism (double exchange mechanism). The detected ferromagnetic behavior could be ascribed to the substitution of Cr ions for Cd ions in the CdSe lattice. Similar behavior of ferromagnetic increase with TM doping was observed by Singh [55] and Kumar [56]. These observations also indicate that the Cr ions systematically substituted for Cd sites without changing the wurtzite structure.

## 4. Conclusions

A series of $Cd_{1-x}Cr_xSe$ (x = 0, 0.02, 0.04, 0.06, 0.08, and 0.10) films were evaporated using electron beam gun technique onto a glass substrates. The XRD analysis for the different compositions of $Cd_{1-x}Cr_xSe$ films shows a polycrystalline with wurtzite structure. The (200) plane is the most dominant preferred orientation seen in all films. In terms of XRD analysis, the lattice constants "a" and "c" are found to be increased with increasing Cr concentration at the expense of Cd. The crystallite size increases and the lattice strain decreases with the increase in Cr content.

The optical properties of the $Cd_{1-x}Cr_xSe$ films were studied in terms of transmittance and reflectance spectrum. The refractive indices were evaluated by Swanepoel's method and found to decrease with increasing Cr content. The optical band gap was determined in strong absorption region of transmittance and reflectance spectrum. It was found to increase with increasing the Cr content in $Cd_{1-x}Cr_xSe$ films. The magnetic measurements displayed room temperature ferromagnetism in all the Cr-doped CdSe samples. The detected ferromagnetic behavior could be ascribed to the substitution of Cr ions for Cd ions in the CdSe lattice.

**Acknowledgments**

The authors gratefully thank the Deanship of Scientific Research at King Khalid University for the financial support through research groups program under grant number (R.G.P.1/57/39). Besides, the authors thank Al-Azhar university for providing the facilities during samples preparation and testing.

## References

[1] S. M. Sze, "Semiconductor Devices: Physics and Technology," 2nd ed. John Wiley & Sons, 1985.
[2] K. N. Shreekanthan, B.V. Rajendra, V. B. Kasturi, G. K. Shivakumar; Cryst. Res. Technol. **38**, 30 (2003).
[3] S. S. Kale, C. D. Lokhande; Materials Chemistry and Physics **62**, 103 (2000).
[4] Y. H. Yu, P. V. Kamat, M. A. Kuno; Adv. Funct. Mater. **20**, 1464 (2010).
[5] V. L. Colvin, M. C. Schlamp, A. P. Alivisatos, Nature **370**, 354 (1994).
[6] N. G. Zakharov, K. V. Vorontsov, Y. N. Frolov, Bulletin of the Lebedev Physics Institute **42**(7), 216 (2015).
[7] Y. Jiang, W. J. Zhang, J. S. Jie, X. M. Meng, X. Fan, S. T. Lee, Adv. Funct. Mater. **17**, 1795 (2007).
[8] Jaeyoung Jang, Dmitriy S. Dolzhnikov, Wenyong Liu, Sooji Nam, Moonsub Shim, Dmitri V. Talapin, Nano Lett. **15**, 6309 (2015).
[9] M. I. Miah, Optical Materials **29**, 845 (2007).
[10] F. Pan, C. Song, X. J. Liu, Y. C. Yang, F. Zeng, Materials Science and Engineering: R: Reports **62**, 1 (2008).
[11] M. Tanaka, Journal of Crystal Growth **278**, 25 (2005).
[12] Y. Ohno, D.K. Young, B. Beschoten, F. Matsukura, H. Ohno, D. D. Awschalom 790 (1999).
[13] C. Liu, F. Yun, H. Morkoç, Materials in Electronics **16**, 555 (2005).
[14] W. Prellier, A. Fouchet, B. Mercey, Journal of Physics: Condensed Matter **15**, R1583 (2003).
[15] K. A. Bogle, S. Ghosh, S. D. Dhole, V.N. Bhoraskar, L.-F. Fu, M.-F. Chi, N. D. Browning, D. Kundaliya, G. P. Das, S. B. Ogale, Chemistry of Materials **20**, 440 (2008).
[16] J. Singh, N. K. Verma, Journal of Superconductivity and Novel Magnetism **25**, 2425 (2012).
[17] T. Dietl, H. Ohno, MRS Bulletin **28**, 714 (2003).
[18] Y. Zhao, Z. Yan, J. Liu, A. Wei, Materials Science in Semiconductor Processing **16**, 1592 (2013).
[19] M. Califano, A. Zunger, A. Franceschetti, Applied Physics Letters **84**, 2409 (2004).

[20] E. Hendry, M. Koeberg, F. Wang, H. Zhang, C. de Mello Donegá, D. Vanmaekelbergh, M. Bonn, Physical Review Letters **96**, 057408 (2006).
[21] R. D. Schaller, M. A. Petruska, V. I. Klimov, Applied Physics Letters **87**, 253102 (2005).
[22] E. Hendry, M. Koeberg, F. Wang, H. Zhang, C. de Mello Donegá, D. Vanmaekelbergh, M. Bonn, Physical Review Letters **96**, 057408 (2006).
[23] M. Emam-Ismail, M. El-Hagary, E. R. Shaaban, S. Althoyaib, J. Alloys Compd. **529**, 113 (2012).
[24] J. Sivasankar, P. Mallikarjana, M. Rigana Begam, N. Madhusudhana Rao, S. Kaleemulla, J. Subrahmanyam, Journal of Materials Science: Materials in Electronics **27**, 2300 (2016).
[25] G. Krishnaiah, N. Madhusudhana Rao, D. Raja Reddy, B. K. Reddy, P. S. Reddy, Journal of Crystal Growth **310**, 26 (2008) DOI: 10.1016/j.jcrysgro.2007.10.013.
[26] S. Neeleshwar, C. L. Chen, C. B. Tsai, Y. Y. Chen, C. C. Chen, S. G. Shyu, M. S. Seehra, Physical Review B **71**, 201307 (2005).
[27] E. R. Shaaban, M. El-Hagary, M. Emam-Ismail, A. Matar, I. S. Yahia, Materials Science and Engineering B **178**, 183 (2013).
[28] H. M. Rietveld, J. Appl. Cryst. **2**, 65 (1969).
[29] B. Cullity, Elements of X-Ray Diffraction (Addison-Wesley, Reading, MA, 1976) pp. 1-80.
[30] B. D. Cullity. Elements of X-ray Diffraction: Addison-Wesley Publishing Company; 1978.
[31] J. I. Langford, J Appl Crystallogr. **11**(2), 102 (1978).
[32] E. R. Shaaban, A. E. Metawa, A Almohammedi, H Algarni, A. M. Hassan, G. A. M. Ali, et al. Mater. Res. Express **5**(8), 086402 (2018).
[33] H. P. Klug, X-ray Diffraction Procedures for Polycrystalline and Amorphous Materials. 2nd ed. New York: John Wiley & Sons; 1974. p. 618–708.
[34] E. R. Shaaban, I. Kansal, S. Mohamed, J. M. Ferreira, Physica B Condens Matter. **404**(20), 3571 (2009).
[35] A. Patterson, Phys Rev. **56**(10), 978 (1939).
[36] E. R. Shaaban, J. Alloys Compd. **563**, 274 (2013).
[37] A. Almohammedi, A. Ashoura, E. R. Shaaban, Chalcogenide Letters **15**, 555 (2018) .
[38] B. D. Cullity, S. R. Stock, Elements of X-Ray Diffraction, 3rd Ed., Prentice-Hall Inc., (2001) 167-171.
[39] R. Swanepoel, J. Phys. E: Sci. Instrum. **17**, 896 (1984).
[40] R. Swanepoel, J. Phps. E: Sci. Instrum. **16**, 1214 (1983).
[41] N. Revathi, P. Prathap, K. T. R. Reddy, Solid State Sciences **11**, 1288 (2009).
[42] A. Purohit, S. Chander, S. Nehra, C. Lal, M. Dhaka, Optical Materials, **47**, 345 (2015).
[43] T. S. Moss, Optical Properties of Semiconductors, Butterworth, London, 1959.
[44] R. Ramırez-Bon, F. J. Espinoza-Beltran, H. Arizpe-Chavez, O. Zelaya-Angel, F. Sanchez-Sinencio, J. Appl. Phys. 77, 5461 (1995).
[45] A. F. Qasrawi, N. M. Gasanly, Semicond. Sci. Technol. **20**, 446 (2005).
[46] M. Tahashi, Z. Wu, H. Goto, Y. Hayashi, T. Ido, Mater Trans. **50**(4), 719 (2009).
[47] P. Mallikarjana, J. Sivasankar, S. Kaleemulla, J. Subrahmanyam, Room J. Nano- Electron. Phys. 8(4 (2)), 04077-1 (2016).
[48] A. Sundaresan, C. N. R. Rao, Nano Today **4**, 96 (2009).
[49] S. B. Singh, M. V. Limaye, S. K. Date, S. K. Kulkarni, Chem. Phys. Lett. **464**, 208 (2008).
[50] L. Saravanan, A. Pandurangan, R. Jayavel, J. Nanopart. Res. **13**, 1621 (2011).
[51] N. H. Hong, J. Sakai, N. T. Huong, Poirot N, Ruyter. Phys. Rev. B. **72**(4), 045336 (2005).
[52] J. Coey, M. Venkatesan, C. Fitzgerald, Nat. Mater. **4**(2), 173 (2005).
[53] S. Ramachandran, J. Narayan, J. Prater. Appl Phys Lett. **88**(24), 242503 (2006).
[54] S. Koshihara, A. Oiwa, M. Hirasawa, S. Katsumoto, Y. Iye, C. Urano, et al. Phys. Rev. Lett. **78**(24), 4617 (1997).
[55] J. Singh, N. Verma, J Supercond Novel Magn. **27**(10), 2371 (2014).
[56] T. R. Kumar, P. Prabukanthan, G. Harichandran, J. Theerthagiri, S. Chandrasekaran, J. Madhavan, Ionics **23**(9), 2497 (2017).